Hybridization of Curvilinear Time-Domain Integral Equation and Time-Domain Optical Methods for Electromagnetic Scattering Analysis

S. P. Walker and Markku J. Vartiainen

***Abstract*—Full-field solutions for scattering and similar problems become prohibitively expensive for electrically large bodies. Fortunately, broadly "optical" methods become accurate as larger bodies are considered. Often, however, large bodies have significant features that are not electrically large and here hybrid approaches are appropriate. In this paper, we present a novel hybridization of time-domain integral equation methods with time-domain physical optics (PO). For both methods, an isoparamteric curvilinear treatment is adopted. The application of the approach is demonstrated by investigating the convergence of the solution for a pulse incident on a large target with a small feature (a 16-pulsewidth plate with a $\sim$1/3-pulsewidth sphere placed centrally just in front of it). It is demonstrated that a full-field solution for the sphere and a fairly small region around the sphere, coupled with the PO solution of the remainder of the plate, produces a converged prediction of the time-dependent fields.**

***Index Terms*—Electromagnetic scattering, transient scattering.**

I. Introduction

THE cost of large electromagnetic scattering computations, for purposes such as electromagnetic pulse (EMP), electromagnetic compatibility (EMC), and radar cross section (RCS), rises sharply with frequency f, varying with anything up to the sixth power. A fuller discussion of this is provided by Miller [1], [2]. One consequence is that full-field solutions on many of the bodies of real interest are way beyond reach.

One approach is to employ one of the wide range of optical methods. Broadly, optical methods are good for bodies of which the length scale is large compared to a wavelength. For problems of the class for which they are suitable, solutions can be obtained at costs some orders of magnitude lower than the cost of full-field solutions. However, many problems combine both a large overall size and important features that are not large compared to a wavelength; optical methods would be inaccurate and field solutions too expensive. It is because of this that there is a considerable body of work addressing the hybridization of various forms of optical treatment with full-field solutions, allowing each to be used for that portion of the body for which it is most suited.

Differential equation approaches are widely used for scattering calculations [3] and there have been hybrid approaches to these [4]. We will restrict ourselves here to integral equation approaches. There have been many reported hybridizations of integral and optical methods in the frequency domain, but none of which we are aware in the time domain. There has been an increased interest in time-domain methods of late, partly because they can exhibit less unfavorable cost scalings than frequency-domain methods and partly because of the advantages of true time-domain modeling for applications such as EMP and EMC studies and for the obtaining of broadband responses with an single analysis. The attractions of time-domain hybrid approaches broadly mirror those of the frequency domain and an extension of hybridization into the time domain seems logical.

In the remainder of Section I, we briefly review the work on hybridization in the frequency domain. Section II describes the present boundary integral-equation time-domain (IETD) treatment, concentrating on those aspects which are especially relevant to the hybridization. Section III describes the hybridization approach adopted and in Section IV, we present results from its application.

An overview of frequency-domain current-based hybrid methods combining physical optics (PO) and moment method (MM) can be found in several fairly comprehensive reviews [5]–[7], so our survey here will be brief.

Hodges and Rahmat–Samii introduce a hybrid method which incorporates PO with a combination of MM solution for electric field integral equation (EFIE) and magnetic field integral equation (MFIE). PO current is introduced as an approximation of the MFIE integral operator. Initially [5] only the "first" contribution from PO region is assumed, whereas later [8], the authors describe an iterative approach with the hybrid code accounting for higher order interactions (e.g., multiple reflections and creeping waves). The iterative technique is applied in the resonance range to a monopole on a cylinder configuration. Although a low-frequency target, results for surface field strengths are in good agreement with experimental data.

Jacobus and Landstorfer [6] solve the EFIE using PO current approximations for three-dimensional (3-D) bodies of arbitrary shape. Time-domain scattering response was investigated by means of Fourier transform in a manner similar to Thiele and Chan [9]. Later [10], Jacobus and Landstorfer extend the technique, accounting for the influence of edges of flat polygonal patches on a body. They use Sommerfeld's solution for calculating exact current density as a summation of a

Manuscript received June 27, 1996; revised March 6, 1997. This work was supported in part by EPSRC, U.K.

The authors are with the Mechanical Engineering Department, Imperial College of Science Technology and Medicine, London, SW7 2BX U.K.

Publisher Item Identifier S 0018-926X(98)02267-4.

PO current and a fringe wave. In later papers [11], [12], a correction term is employed for PO current close to wedges based on the uniform theory of diffraction (UTD) [13]. In those papers, code verification was by comparing hybrid results for low-frequency solutions using MM for geometries such as a sphere, a dipole-sphere, and a cube.

Medgyesi–Mitschang and Wang [14] apply PO-MM hybrid formulation in asymptotic regions of bodies of revolution. They solve EFIE formulation by incorporating optically derived Ansatz solutions for surface currents of the scatterer. The MM is thus hybridized with currents derived by Fock theory [15] or PO. The hybrid technique was applied to a sphere and to cone spheres. Results were compared with MM solutions and their technique using both PO-MM and Fock-MM approaches appears to be accurate for scatterers in the near-resonance range.

II. Time-Domain Integral Equation Treatment

Derivations of the MFIE are presented in several references [16]. Here, we will only quote it for scattering from a perfectly conducting body subject to some incident wave with the $\boldsymbol{H}$ field at some location $\boldsymbol{r}$ on the surface given in terms of an integral of the history of the field over all other (primed) surface locations

$$2\pi \boldsymbol{H}(\boldsymbol{r},t) = 4\pi \boldsymbol{H}_{\rm inc}(\boldsymbol{r},t) + \int_{\partial\Omega} (\boldsymbol{n}' \times \boldsymbol{H}(\boldsymbol{r}',t^*)) \times \frac{\hat{\boldsymbol{R}}}{R^2} + \left(\hat{\boldsymbol{n}}' \times \frac{\partial \boldsymbol{H}}{\partial t'};(\boldsymbol{r}',t^*)\right) \times \frac{\hat{\boldsymbol{R}}}{cR}\, ds' \quad (1)$$

We will (in later discussion) refer to the point $\boldsymbol{r}$ at which the field is being found as the field point or node; contributions to this field will come from integrations over boundary points or nodes at $\boldsymbol{r}'$ on s'. Time is t and t^* is retarded time. We solve for the surface $\boldsymbol{H}$ field rather than the surface current $\boldsymbol{n} \times \boldsymbol{H}$ (although either approach can be used and the hybridization is unaffected). The vector from $\boldsymbol{r}$ to $\boldsymbol{r}'$ we denote $\boldsymbol{R}$.

The surface is divided into M quadrilateral elements. We perform a local curvilinear transformation of these curved patches into flat bi-unit squares in intrinsic space via polynomial shape functions with an associated isoparametric representation of field variables *inter alia* providing a continuous surface field. The temporal variation is similarly treated. The integrations are then performed using Gaussian quadrature. This whole process is presented more fully elsewhere [17].

We arrive at the discretized form, giving the field at a particular one of the N nodes

$$2\pi \boldsymbol{H}_i^k = 4\pi \boldsymbol{H}_{{\rm inc},i}^k + \sum_{m=1}^{M} \sum_{\alpha} \sum_{\beta} [K] H_j^{k^*}. \quad (2)$$

Here, the nested summations are over elements and then temporal and spatial shape functions within elements. The matrix $\boldsymbol{K}$ is the result of integrating (via Gaussian quadrature) the kernels of (1) over each element. In practice, there is yet one further nested summation over partitions of elements; some weakly singular and some hypersingular integrals require additional partitioning of the elements. This is described more fully in the references cited and elsewhere [17], [18]. The work involved in using (2) can be identified as follows.

1) The main system matrix resulting from integration over each element, "from" each of the N nodes, in turn, must be formed. This has a cost scaling with N^2 (i.e., with frequency f to the fourth power).
2) At each timestep, the summations must be evaluated. This process may be interpreted here as a large matrix-vector multiplication; the main system matrix multiplying historical values of surface field. For each node, contributions from N other nodes must be considered, giving a cost scaling with N^2 at each timestep. With the number of timesteps needed itself typically scaling with the body size (i.e., $\sim N^{1/2}$), this yields an overall cost scaling with f^5. For sizeable problems, this is the dominant cost component in the method.

Later discussion of the hybrid approach will be helped by consideration of a diagrammatic representation of this. The position is rather more complicated for the implicit formulation actually adopted. Further, the smooth quadratic modeling of the temporal variation used results in the main system matrix actually being in size $N \times N \times \sim 6$ as the historical value at some retarded time is, in general, a weighted sum of values at a number of neighboring timesteps. Both of these complications can be safely ignored for present purposes; the representation below is for an explicit treatment with "constant" time elements

$$\begin{bmatrix} \\ \boldsymbol{H} \\ \\ \end{bmatrix} = \begin{bmatrix} \\ \boldsymbol{H}_{\rm inc} \\ \\ \end{bmatrix} + \begin{bmatrix} s & y & s & t & m \\ & & & & \\ & & & & \\ & & & & \\ m & a & t & r & x \end{bmatrix} \begin{bmatrix} h & h & h & h & h \\ i & i & i & i & i \\ s & s & s & s & s \\ t & t & t & t & t \\ 1 & 2 & \cdot & \cdot & N \end{bmatrix}. \quad (3)$$

Note that here the equivalent of the single vector of unknowns in the frequency-domain case is actually a set of N vectors of historical surface field values. Each row of the system matrix operates on a different one of these with the members of each history vector being the historical values at the retarded times appropriate for the node pair at issue. The most recent members of these vectors are those operated on by the diagonal members of the matrix and are the new field values sought for the present timestep.

As mentioned, the above discussion is for an explicit treatment. In practice, instabilities result unless an implicit treatment (or some less accurate averaging process) is used [17], [19]. An implicit method has other major advantages, both of accuracy and of cost saving by avoiding the need to constrain the timestep to suit the smallest nodal spacing. The summation process of (2) above is actually the formation of the "right-hand side" for the sparse matrix equation to be solved at each timestep; it is as this that we will refer to it subsequently. Again, further details are available in the references cited.

Equations (1)–(3) provide approximations to the surface fields; if the scattered fields are of interest, they are obtained as a postprocessing activity by integration over these surface fields.

III. Time-Domain Hybridization

Consider the 3-D body where we have identified that region (I) where the local geometry requires a full-field solution and that (II) where time domain PO will be used. We will take the fraction of nodes falling within (I) to be θ. For subsequent convenience in illustration, we will take the regions to comprise consecutively numbered nodes, but this is not necessary.

It is helpful to consider the consequences of this in terms of system matrix sizes and shapes, to identify the main computational cost components, and opportunities for their reduction.

The discussion is most readily approached via a brief consideration of the issues in the simpler frequency domain. We would then have had a matrix of the following form:

$$\left[\begin{array}{c|c} A & B \\ \hline C & D \end{array}\right] \left[\underline{\boldsymbol{H}}\right] = \left[\underline{\boldsymbol{H}}_{\mathrm{inc}}\right]. \tag{4}$$

Fractions θ and $(1-\theta)$ of columns lie in A and B, respectively, and similarly rows in A and C. We would only ever form (2) for nodes in (I)—regions A and B of the matrix. Regions C and D are never formed. Values of $\boldsymbol{H}$ in (II), the lower part of the column, are known from the PO solution; these are simply multiplied by portion B and taken to the right-hand side. We are left with only matrix region A to solve. The main cost components are thus of order θN^2 (forming the A and B portions) and $\theta^3 N^3$—the generally still dominant cost of solving the remaining matrix A. The cost in the frequency domain thus falls with the (inverse) cube of the fraction, which must be treated by the integral equation; equivalently, the cost of the integral equation analysis scales with the cube of the number of nodes involved, as usual.

We turn now to the time domain, where the cost scaling and cost saving issues are less straightforward. Our objective is still to obtain approximations to the surface fields. For region II this is simple; the surface $\boldsymbol{H}$ field at any location and time is given by the PO approximation

$$\boldsymbol{H}(\boldsymbol{r},t) = -2\boldsymbol{n} \times (\boldsymbol{n} \times \boldsymbol{H}_{\mathrm{inc}}(\boldsymbol{r},t)) \tag{5}$$

where the discretization adopted retains a continuous field distribution at the interface of the regions just as it does elsewhere. For nodes within region I we apply (1), which shows the field "here and now" to be a simple geometrically weighted integral of earlier surface fields over all the rest of the body. Partitioning the domain of integration of (1) into regions I and II we have

$$\begin{aligned} 2\pi\boldsymbol{H}(\boldsymbol{r},t) = {} & 4\pi\boldsymbol{H}_{\mathrm{inc}}(\boldsymbol{r},t) + \int_{\partial\Omega_I} (\boldsymbol{n}' \times \boldsymbol{H}(\boldsymbol{r}',t^*)) \\ & \times \frac{\hat{\boldsymbol{R}}}{R^2} + \left(\boldsymbol{n}' \times \frac{\partial \boldsymbol{H}}{\partial t'}(\boldsymbol{r}',t^*)\right) \times \frac{\hat{\boldsymbol{R}}}{cR}\, ds' \\ & + \int_{\partial\Omega_{II}} (\boldsymbol{n}' \times \boldsymbol{H}(\boldsymbol{r}',t^*)) \\ & \times \frac{\hat{\boldsymbol{R}}}{R^2} + \left(\boldsymbol{n}' \times \frac{\partial \boldsymbol{H}}{\partial t'}(\boldsymbol{r}',t^*)\right) \times \frac{\hat{\boldsymbol{R}}}{cR}\, ds'. \end{aligned} \tag{6}$$

As in the frequency-domain case, we simply do not form an equation for nodes in II.

For nodes in I the field is found from the usual integrations over the IETD region I plus the integrations over the optical region II. This integration is of known quantities and, thus, can readily be evaluated. In terms of (6), it can be interpreted as an addition to the incident wave term. For region II, this integration requires that for each of θN nodes we multiply out $(1-\theta)N$ matrix coefficients and field values, resulting in an overall cost a factor $\theta - 1$ lower than the fully IETD approach. This is obviously as yet much less attractive than the θ^{-3} factor saving in the frequency domain. However, for harmonic illumination, each surface-field value in region II will oscillate sinusoidally. Because of this, the result of any integration over this portion of the surface from any field node will, itself, oscillate harmonically. (Equivalently, for a pulsed incident wave the short-pulse duration provides similar time saving.) The consequence is that for any field node in II, the integration over the surface I need be performed for one half of one period; subsequent integrations will merely duplicate this result. The cost of these integrations will vary with $\sim\theta N^2$ and be a modest multiple of the equivalent activity in the frequency-domain case. It is a cost scaling with frequency to the fourth power. The treatment otherwise of region I is as normal with a cost θN^2 per timestep.

The overall cost then depends on the number of timesteps for which the IETD analysis must be performed. If it is necessary to model for a transit time of the whole body we have an overall cost of $\theta^2 N^{5/2}$ or $\theta^2 f^5$. It could be that effects on region I from parts of region II very remote from region I can be neglected and that a modeling duration of a few transit times of the IETD region I is acceptable. If so, the overall cost is correspondingly reduced.

In terms of matrix manipulations we have a modification of (3) above [where the single history vector is to be taken to represent the multiple ones of (3)]

$$\left[\underline{\boldsymbol{H}}\right] = \left[\underline{\boldsymbol{H}}_{\mathrm{inc}}\right] + \left[\begin{array}{c|c} A & B \\ \hline C & D \end{array}\right] \left[\underline{\boldsymbol{H}}_{\mathrm{hist}}\right]. \tag{7}$$

IV. Results

One difficulty with such a treatment is in finding suitable test cases to validate the implementation; if they are small enough to be calculable by other means, they are too small for the hybrid approach to be expected to perform well. We have adopted a three-stage approach to validation and demonstration. The time-domain PO implementation has been investigated in isolation with no IETD region. No results are given here, but behavior is as expected; for example, results on large spheres tend toward analytical results. The efficacy of the hybridization is demonstrated, by analysis of a problem small enough to be soluble by a full-field solution (and, thus, a problem for which the hybrid is of little practical benefit) and for which an analytical solution exists. Finally, for a problem too large to be treated by a full-field solution and for which we have no analytical solution, we demonstrate the convergence of the hybrid result as the IETD region I is increased in size.

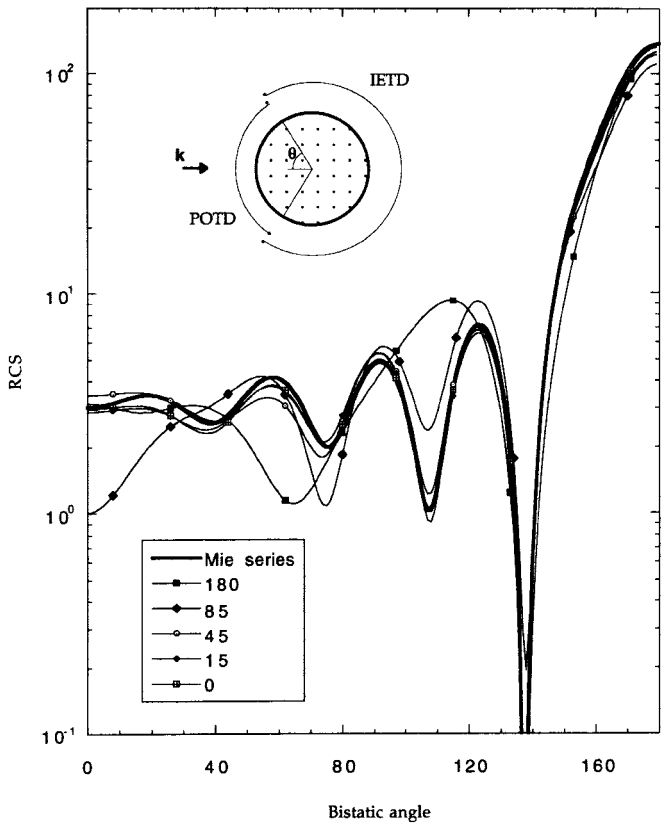

Fig. 1. Bistatic $\boldsymbol{E}$-plane RCS of a two wavelength sphere calculated via: the Mie series, wholly IETD, wholly POTD, and three IETD/POTD hybrid approaches. The size of the POTD regions is defined by the angle θ in degrees its radius subtends at the center.

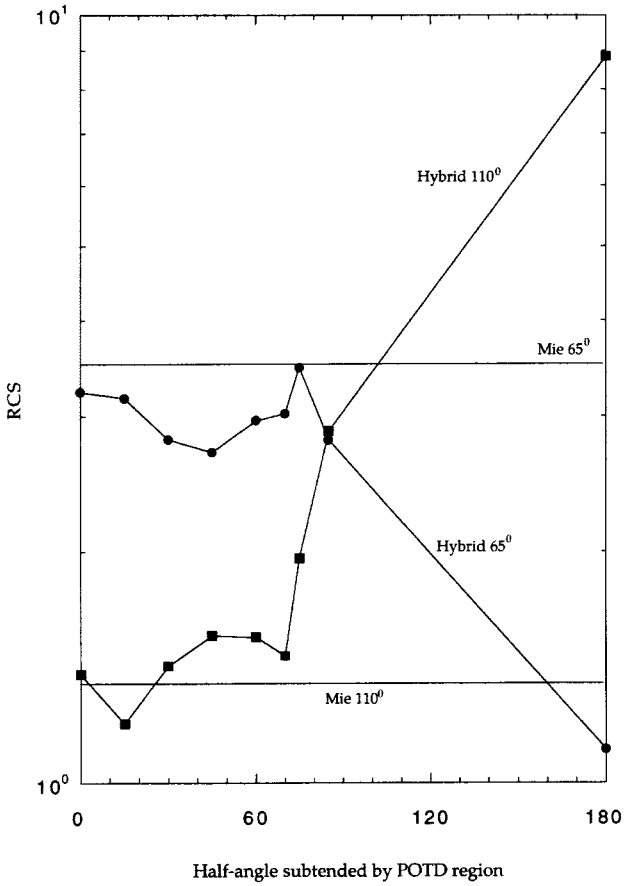

Fig. 2. RCS at bistatic angles of 65° and 110° versus the (half) angular extent of the POTD region. Corresponding exact Mie series results also shown.

A. Correctness of Hybridization

Fig. 1 shows the bistatic rcs of a two-wavelength (1282 node) diameter sphere calculated by the Mie series and a set of hybrid analyses in which different fractions of the surface were analyzed using POTD with the balance employing the full IETD. The extent of the POTD region is characterized by the half angle it subtends, as indicated in the inset in Fig. 1.

With no POTD region (the "zero degrees" case) the agreement between the Mie series and the wholly IETD solution is good. As the extent of the POTD region is increased, the accuracy of the solution generally declines. In Fig. 2 we consider in more detail two bistatic angles, 65° and 110°, at which the wholly POTD (180° half angle) case differs markedly from the Mie series solution. We show the change in RCS as the POTD region is reduced from a 180° degree half angle in stages to end with a wholly IETD solution. A general reduction in error as the increasingly IETD solution is employed is seen.

While use on such a target is of no practical interest as the cost of a full-field solution is anyway trivial, it indicates that the hybridization itself is performing in a satisfactory manner.

B. Convergence Study

We now analyze a large problem for which no analytical solution is available. We consider a unit radius sphere placed centrally 1.75 diameters in front of a square plate of side 50 diameters. This arrangement is shown in Fig. 3. Lettered locations on the side view indicate points on the surface of the sphere at which results are extracted or mentioned. Similarly, fields computed at the set of locations indicated on the plate vertically below the sphere will also be plotted. This assembly is just such as requires a hybrid treatment, with the length scales of the plate and sphere so different. A full-field solution would be prohibitively expensive for a case with the pulse width of order the sphere diameter, but for this same case an optical treatment of the sphere and its immediate surroundings would be very inaccurate. Here, we will treat via IETD the sphere itself and various circular regions of the plate directly behind the sphere centered on the sphere axis.

We illuminate from a direction 6° off-normal, with an incident wave given by

$$\boldsymbol{H}_{\mathrm{inc}}(\boldsymbol{r},t) = \boldsymbol{H}_0 \exp\left\{\frac{4\ln 2\left(t-\dfrac{R}{c}\right)^2}{g^2}\right\}. \tag{8}$$

The pulse-width parameter g is selected to make the width at half maximum of this pulse 2.75 sphere diameters.

We investigate the behavior of the solution as the diameter of the circular IETD region is changed. It is to be expected that as the diameter of the IETD region is increased, the results will change until the IETD region has encompassed locations

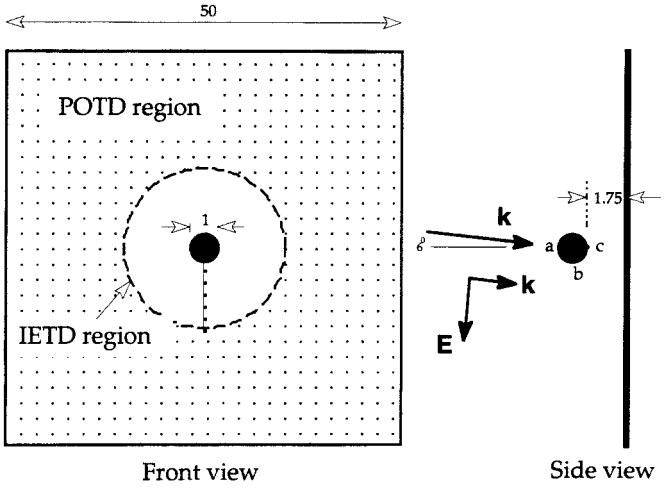

Fig. 3. Sphere and plate arrangement, showing incident wave, the IETD and POTD regions, and various observation locations.

where the field is significantly perturbed by the sphere in ways which have in turn a significant effect on some particular location of interest.

Fig. 4 shows the $\boldsymbol{H}$ field magnitude at location (a) for:

1) the diameter of the IETD region on the plate set to 6.5 sphere diameters, the biggest IETD region studied (continuous line);
2) the diameter of the IETD region on the plate set to zero with just the sphere treated by IETD and all the plate treated by POTD (black circles, no line);
3) a wholly POTD solution (dashed line).

The wholly POTD solution is grossly inaccurate, with the second peak as the reflected wave passes (a) naturally not captured. Both of the hybrid cases do capture it and, indeed, their predictions are very similar. The smooth oscillatory behavior just after the second large peak, which the larger IETD region case predicts, is not predicted by the case with only the sphere analyzed via IETD. Nonetheless, even here the difference is only about 4% of the peak field. Figures are not shown, but very similar observations could be made concerning behavior at locations (b) and (c).

Both hybrid cases capture the secondary peak at about $t = 2$, postdating the main pulse by one transit time from the plate edge to the sphere. Naturally, this also is not predicted by the POTD treatment. (Note that in Fig. 4 the actual time dependence is in all cases smoother than the figure indicates. The graphs are plotted with straight lines joining values at timesteps; the actual analysis uses quadratic temporal elements.)

Fig. 5 is an attempt to show the degree of convergence in the results as the IETD region is increased. On the horizontal axis is plotted the area of the IETD region. The first point $(\text{area} = 0)$ corresponds to a wholly POTD solution; the second $(\text{area} = 3.14)$ corresponds to just the sphere being treated by IETD; other cases are for the sphere and, in addition, circular regions on the plate of increasing size being treated by IETD. On the vertical axis is plotted $\boldsymbol{H}$ field magnitude for a set of times corresponding to the occasions of largest difference between the maximum IETD and wholly POTD solutions.

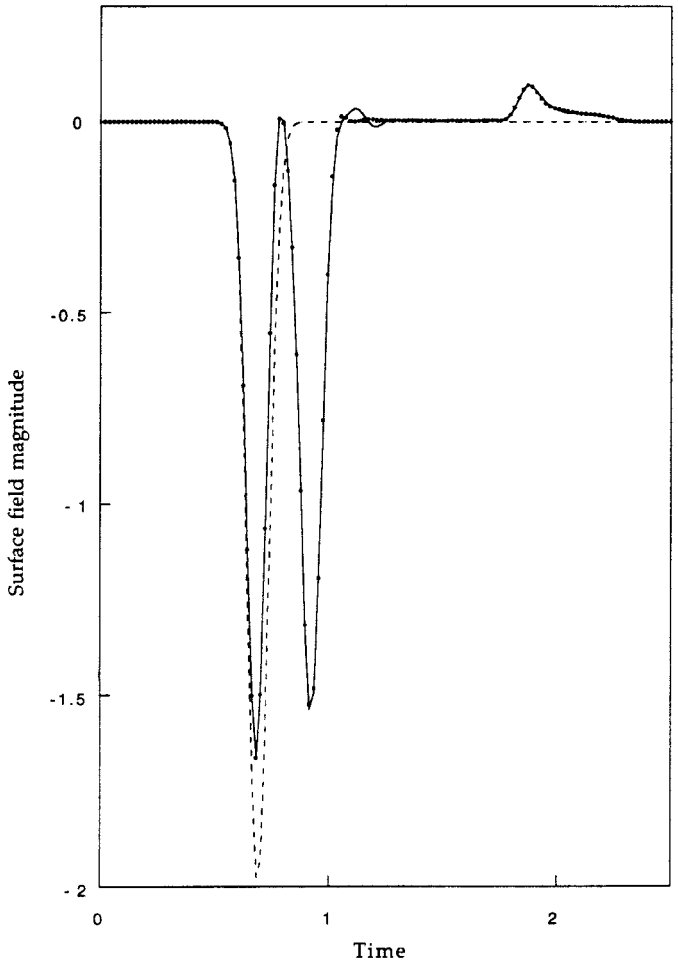

Fig. 4. $\boldsymbol{H}$ field magnitude versus time at location (a) (indicated in Fig. 3) for various extents of IETD region. Dotted line: POTD throughout. Solid line: IETD region diameter 6.5 sphere diameters. Individual circular points: IETD on all the sphere, POTD on the plate.

These times are the two large negative peaks, the positive peak at time $\sim$1.1, and the later positive peak at $\sim$2. Each of these times is represented by a line on the graph. It is clear that the result is converging as the diameter of the IETD region is increased and that for most practical purposes, the converged solution is obtained with a relatively small region treated by IETD.

Such convergence might be expected to be associated with inclusion in the IETD region of all of the surface where the field is significantly influenced by the presence of the sphere; elsewhere, the POTD provides a good approximation. We investigate this by examining the plate surface $\boldsymbol{H}$ field at the series of points radially along the E direction indicated in Fig. 3.

The time-dependent $\boldsymbol{H}$ field magnitude at these points, calculated using an IETD region 13 sphere diameters in diameter (the biggest studied), is shown in Fig. 6. The locations of the points, in sphere diameters from the axis, are indicated on the figure. Note that the final point is outside the IETD region and, thus, the field there is the POTD field.

To provide scale, the inset shows the field for the full duration with fields at only locations 0.0 and 6.775 (the

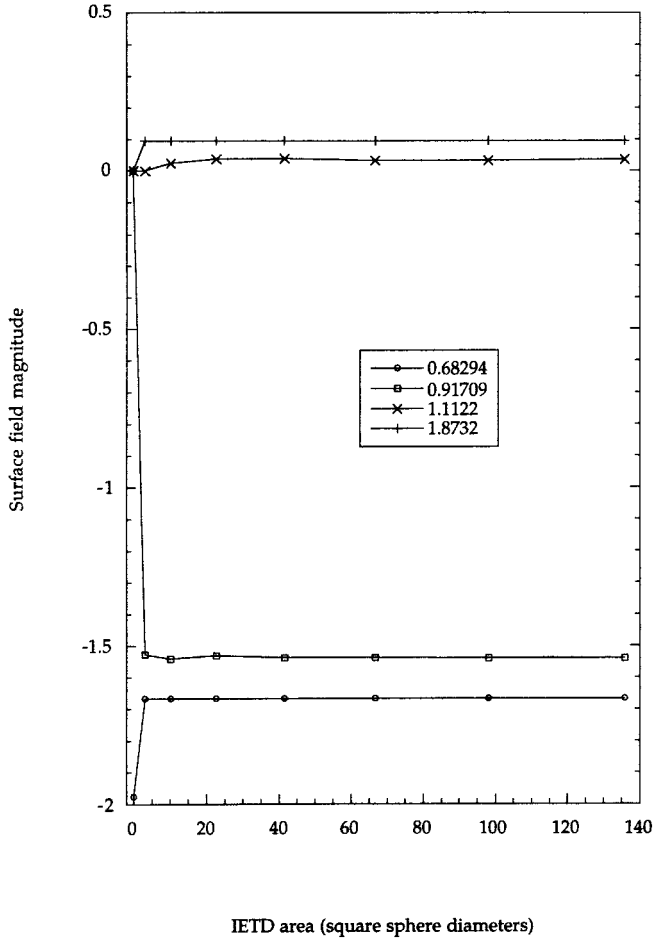

Fig. 5. $\boldsymbol{H}$ field magnitude at location (a) (indicated in Fig. 3) versus the areal extent of the IETD region. Results shown for the four times indicated.

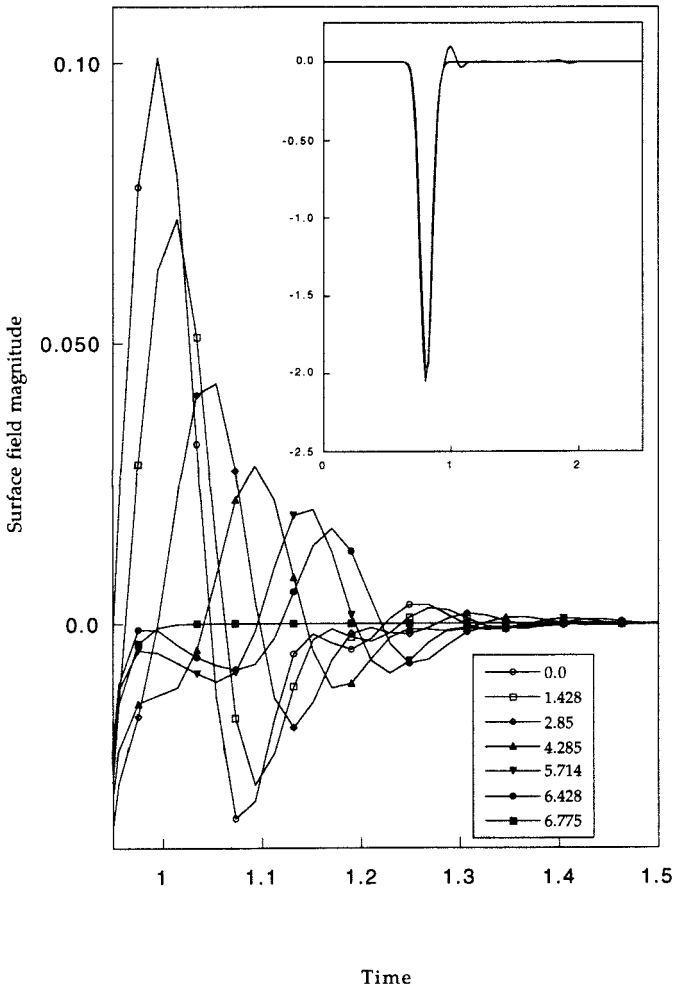

Fig. 6. Time-dependent surface $\boldsymbol{H}$ field magnitude calculated with an IETD region of 6.5 diameters. Field shown at indicated distances in sphere diameters from the axis in the $\boldsymbol{E}$ direction (locations indicated on Fig. 3).

POTD field) shown to avoid excessive clutter. The main part of Fig. 6 concentrates on a zoomed view of the period just after the primary pulse when a small secondary pulse is evident. This pulse is a consequence of the perturbation by the sphere of what would otherwise be the PO field on the plate due to the incident pulse. It is seen that as locations further from the sphere are considered the height of the secondary pulse falls steadily. For the furthest off-axis IETD location (6.428 diameters) this secondary pulse height is only about 1% of the peak field magnitude. This compares to about 5% at the most central location with intermediate locations showing a steady gradation between these values. The associated temporal shift between these cases is a consequence of the progressively longer time required for the perturbation due to the sphere to propagate out to the progressively more distant locations. Naturally, there is no radius at which the perturbation is literally nonexistant, but these observations, that by the $\sim$6.5 diameters studied here the field is very little different from the unperturbed field, support the observations regarding convergence made earlier.

V. Conclusions

The extension of integral equation hybrid methods into the time domain has been demonstrated.

For the small sphere where an analytical solution is available, convergence of the hybrid to the analytical solution is observed as the region treated via IETD is increased.

The plate and sphere problem is large; a wholly integral equation treatment would be impractical and a wholly optical treatment would not even be qualitatively correct. The hybrid approach developed seems well able to deal with the problem; the behavior expected qualitatively is observed and convergence is obtained as the IETD region is increased. The actual computational cost saving is naturally highly problem dependent and would, for example, be even larger for a larger plate. Here, for even the largest IETD region studied, costs are reduced relative to what they would be for a wholly IETD solution by about two orders of magnitude. The approach seems capable of yielding the time-dependent fields on large bodies with locally small features.

Acknowledgment

The authors would like to thank Dr. M. Bluck and Dr. M. D. Pocock of the Department of Mechanical Engineering, Imperial College of Science Technology and Medicine, London, U.K., for their helpful discussions.

REFERENCES

[1] E. K. Miller, "Time-domain modeling in electromagnetics." *J. Electromagn. Waves Applicat.*, vol. 8, pp. 1125–1172, 1978.

[2] ———, "A selective survey of computational electromagnetics," *IEEE Trans. Antennas Propagat.*, vol. 36, pp. 1281–1305, Sept. 1988.

[3] A. Taflove, *Computational Electromagnetics; The Finite Difference Time Domain Method*. Boston, MA: Artech House, 1995.

[4] T. T. Chia, R. J. Burkholder, and R. Lee, "The application of FDTD hybrid methods for cavity scattering analysis," *IEEE Trans. Antennas Propagat.*, vol. 43, pp. 1082–1090, Oct. 1995.

[5] R. E. Hodges and Y. Rahmat-Samii, Theory of physical optics hybrid method (POHM), in *Int Symp. Dig.: Antennas Propagat.*, 1994, vol. 2, pp. 1374–1377.

[6] U. Jakobus and F. M. Landstorfer, "Current-based hybrid moment method analysis of electromagnetic radiation and scattering problems," *Appl. Computat. Electromagn. Soc. J.*, vol. 10, pp. 38–39, 1995.

[7] L. N. Medgyesi-Mitschang and D.-S. Wang, "Hybrid methods in computational electromagnetics: A review," *Comput. Phys. Commun.*, vol. 68, no. 1/3, pp. 76–94, 1991.

[8] R. E. Hodges and Y. Rahmat-Samii, "Iterative improvement of physical optics hybrid method—POHM iterative," *IEEE Antennas Propagat. Soc. AP-S Int. Symp.*, 1995, vol. 3, pp. 1460–1463.

[9] G. A. Thiele and G. K. Chan, "Application of the hybrid technique to time domain problems," *IEEE Trans. Antennas Propagat.*, vol. 26, pp. 151–155, Jan. 1978.

[10] U. Jakobus and F. M. Landstorfer, "Improved PO-MM hybrid formulation for scattering from three-dimensional perfectly conducting bodies of arbitrary shape," *IEEE Trans. Antennas Propagat.*, vol. 43, pp. 162–169, Feb. 1995.

[11] ———, "Improvement of the PO-MoM hybrid method by accounting for effects of perfectly conducting wedges," *IEEE Trans. Antennas Propagat.*, vol. 43, pp. 1123–1129, Oct. 1995.

[12] ———, "Correction of the PO current density close to perfectly conducting wedges by the UTD," *Electron. Lett.*, vol. 30, pp. 2111–2112, 1994.

[13] R. G. Kouyoumjian and P. H. Pathak, "A uniform geometrical theory of diffraction for an edge in a perfectly conducting surface," *Proc. IEEE*, vol. 62, pp. 1448–1461, 1974.

[14] L. N. Medgyesi-Mitschang and D.-S. Wang, "Hybrid solutions for scattering from perfectly conducting bodies revolution," *IEEE Trans. Antennas Propagat.*, vol. 31, pp. 570–583, July 1983.

[15] V. A. Fock, *Electromagnetic Diffraction and Propagation Problems, Intenational Series of Monographs on Electromagnetic Waves*. Oxford, U.K.: Pergamon, 1965.

[16] A. J. Poggio and E. K. Miller, "Integral equation methods of three-dimensional scattering problems," in *Computer Techniques for Electromagnetics*, R. Mittra, Ed. Oxford, U.K.: Pergamon, 1973, pp. 159–265.

[17] M. J. Bluck and S. P. Walker, "Time domain BIE analysis of large three-dimensional electromagnetic scattering problems," *IEEE Trans. Antennas Propagat.*, vol. 45, pp. 894–901, May 1997.

[18] M. J. Bluck, M. D. Pocock, and S. P. Walker, "An accurate method for the calculation of singular integrals arising in time-domain integral equation analysis of electromagnetic scattering," *IEEE Trans. Antennas Propagat.*, vol. 45, pp. 1793–1798, Dec 1997.

[19] P. D. Smith, "Instabilities in time marching methods for scattering: Cause and rectification," *Electromagn.*, vol. 10, pp. 439–451, 1990.

S. P. Walker, for photograph and biography, see p. 146 of the January 1997 issue of this TRANSACTIONS.

Markku Vartiainen received the M.Sc. degree from Helsinki University of Technology, Finland, in 1994. He is currently working toward the Ph.D. degree at Imperial College, London, U.K.

From 1994 to 1995, he was with the Technical Research Center of Finland, Helsinki. His current research interests are in the area of numerical methods in wave propagation, hypersingular integration, and computational vector and tensor algebra.

Mr. Vartiainen was awarded the Academy of Finland Scholarship in 1995.